Research Article | Vol. 8, No. 1 | 1 Jan 2017 | BIOMEDICAL OPTICS EXPRESS 177

Biomedical Optics EXPRESS

Modulation of cardiomyocyte activity using pulsed laser irradiated gold nanoparticles

LARA GENTEMANN,[1,2,6] STEFAN KALIES,[2,3,4,6,*] MICHELLE COFFEE,[4,5] HEIKO MEYER,[1] TAMMO RIPKEN,[1] ALEXANDER HEISTERKAMP,[1,2,3,4] ROBERT ZWEIGERDT,[4,5] AND DAG HEINEMANN[1,2]

[1]*Biomedical Optics Department, Laser Zentrum Hannover e.V., Hollerithallee 8, 30419 Hannover, Germany*
[2]*Lower Saxony Centre for Biomedical Engineering, Implant Research and Development, Stadtfelddamm 34, 30625 Hannover, Germany*
[3]*Institut für Quantenoptik, Gottfried Wilhelm Leibniz Universität Hannover, Welfengarten 1, 30167 Hannover, Germany*
[4]*Cluster of Excellence REBIRTH, Hannover, Germany*
[5]*Leibniz Research Laboratories for Biotechnology and Artificial Organs (LEBAO), REBIRTH - Center for Regenerative Medicine, Department of Cardiothoracic, Transplantation and Vascular Surgery, Hannover Medical School, Carl-Neuberg-Str. 1, 30625 Hannover, Germany*
[6]*These authors contributed equally to this publication and should be considered co-first authors*
[*]*kalies@iqo.uni-hannover.de*

Abstract: Can photothermal gold nanoparticle mediated laser manipulation be applied to induce cardiac contraction? Based on our previous work, we present a novel concept of cell stimulation. A 532 nm picosecond laser was employed to heat gold nanoparticles on cardiomyocytes. This leads to calcium oscillations in the HL-1 cardiomyocyte cell line. As calcium is connected to the contractility, we aimed to alter the contraction rate of native and stem cell derived cardiomyocytes. A contraction rate increase was particularly observed in calcium containing buffer with neonatal rat cardiomyocytes. Consequently, the study provides conceptual ideas for a light based, nanoparticle mediated stimulation system.

OCIS codes: (000.1430) Biology and medicine; (190.4870) Photothermal effects; (350.4855) Optical tweezers or optical manipulation.

References and links

1. X. Huang, P. K. Jain, I. H. El-Sayed, and M. A. El-Sayed, "Gold nanoparticles: interesting optical properties and recent applications in cancer diagnostics and therapy," Nanomedicine (Lond.) **2**(5), 681–693 (2007).
2. H. Jans and Q. Huo, "Gold nanoparticle-enabled biological and chemical detection and analysis," Chem. Soc. Rev. **41**(7), 2849–2866 (2012).
3. X. Huang, P. K. Jain, I. H. El-Sayed, and M. A. El-Sayed, "Plasmonic photothermal therapy (PPTT) using gold nanoparticles," Lasers Med. Sci. **23**(3), 217–228 (2008).
4. Z. Qin and J. C. Bischof, "Thermophysical and biological responses of gold nanoparticle laser heating," Chem. Soc. Rev. **41**(3), 1191–1217 (2012).
5. D. Heinemann, M. Schomaker, S. Kalies, M. Schieck, R. Carlson, H. Murua Escobar, T. Ripken, H. Meyer, and A. Heisterkamp, "Gold nanoparticle mediated laser transfection for efficient siRNA mediated gene knock down," PLoS One **8**(3), e58604 (2013).
6. S. Kalies, D. Heinemann, M. Schomaker, H. Murua Escobar, A. Heisterkamp, T. Ripken, and H. Meyer, "Plasmonic laser treatment for Morpholino oligomer delivery in antisense applications," J. Biophotonics **7**(10), 825–833 (2014).
7. E. Boulais, R. Lachaine, A. Hatef, and M. Meunier, "Plasmonics for pulsed-laser cell nanosurgery: Fundamentals and applications," J. Photochem Photobiol. **17**, 26–49 (2013).
8. J. Krawinkel, U. Richter, M. L. Torres-Mapa, M. Westermann, L. Gamrad, C. Rehbock, S. Barcikowski, and A. Heisterkamp, "Optical and electron microscopy study of laser-based intracellular molecule delivery using peptide-conjugated photodispersible gold nanoparticle agglomerates," J. Nanobiotechnology **14**(1), 2 (2016).
9. C. Hrelescu, J. Stehr, M. Ringler, R. A. Sperling, W. J. Parak, T. A. Klar, and J. Feldmann, "DNA Melting in Gold Nanostove Clusters," J. Phys. Chem. C **114**(16), 7401–7411 (2010).
10. J. Yong, K. Needham, W. G. A. Brown, B. A. Nayagam, S. L. McArthur, A. Yu, and P. R. Stoddart, "Gold-nanorod-assisted near-infrared stimulation of primary auditory neurons," Adv. Healthc. Mater. **3**(11), 1862–1868 (2014).

#274423 http://dx.doi.org/10.1364/BOE.8.000177
Journal © 2017 Received 26 Aug 2016; revised 3 Nov 2016; accepted 11 Nov 2016; published 8 Dec 2016

Biomedical Optics EXPRESS

11. C. Paviolo, A. C. Thompson, J. Yong, W. G. A. Brown, and P. R. Stoddart, "Nanoparticle-enhanced infrared neural stimulation," J. Neural Eng. **11**(6), 065002 (2014).
12. P. Kohl, "Heterogeneous cell coupling in the heart: an electrophysiological role for fibroblasts," Circ. Res. **93**(5), 381–383 (2003).
13. A. Klimas and E. Entcheva, "Toward microendoscopy-inspired cardiac optogenetics in vivo: technical overview and perspective," J. Biomed. Opt. **19**(8), 080701 (2014).
14. T. Bruegmann, D. Malan, M. Hesse, T. Beiert, C. J. Fuegemann, B. K. Fleischmann, and P. Sasse, "Optogenetic control of heart muscle in vitro and in vivo," Nat. Methods **7**(11), 897–900 (2010).
15. Z. Jia, V. Valiunas, Z. Lu, H. Bien, H. Liu, H. Z. Wang, B. Rosati, P. R. Brink, I. S. Cohen, and E. Entcheva, "Stimulating cardiac muscle by light: cardiac optogenetics by cell delivery," Circ Arrhythm Electrophysiol **4**(5), 753–760 (2011).
16. N. I. Smith, Y. Kumamoto, S. Iwanaga, J. Ando, K. Fujita, and S. Kawata, "A femtosecond laser pacemaker for heart muscle cells," Opt. Express **16**(12), 8604–8616 (2008).
17. M. W. Jenkins, A. R. Duke, S. Gu, H. J. Chiel, H. Fujioka, M. Watanabe, E. D. Jansen, and A. M. Rollins, "Optical pacing of the embryonic heart," Nat. Photonics **4**(9), 623–626 (2010).
18. G. Nagel, T. Szellas, W. Huhn, S. Kateriya, N. Adeishvili, P. Berthold, D. Ollig, P. Hegemann, and E. Bamberg, "Channelrhodopsin-2, a directly light-gated cation-selective membrane channel," Proc. Natl. Acad. Sci. U.S.A. **100**(24), 13940–13945 (2003).
19. N. I. Smith, K. Fujita, T. Kaneko, K. Katoh, O. Nakamura, S. Kawata, and T. Takamatsu, "Generation of calcium waves in living cells by pulsed-laser-induced photodisruption," Appl. Phys. Lett. **79**(8), 1208 (2001).
20. N. Khlebtsov and L. Dykman, "Biodistribution and toxicity of engineered gold nanoparticles: a review of in vitro and in vivo studies," Chem. Soc. Rev. **40**(3), 1647–1671 (2011).
21. S. Kalies, G. C. Antonopoulos, M. S. Rakoski, D. Heinemann, M. Schomaker, T. Ripken, and H. Meyer, "Investigation of biophysical mechanisms in gold nanoparticle mediated laser manipulation of cells using a multimodal holographic and fluorescence imaging setup," PLoS One **10**(4), e0124052 (2015).
22. K. Dolnikov, M. Shilkrut, N. Zeevi-Levin, S. Gerecht-Nir, M. Amit, A. Danon, J. Itskovitz-Eldor, and O. Binah, "Functional properties of human embryonic stem cell-derived cardiomyocytes: intracellular Ca2+ handling and the role of sarcoplasmic reticulum in the contraction," Stem Cells **24**(2), 236–245 (2006).
23. H. Kempf, C. Kropp, R. Olmer, U. Martin, and R. Zweigerdt, "Cardiac differentiation of human pluripotent stem cells in scalable suspension culture," Nat. Protoc. **10**(9), 1345–1361 (2015).
24. H. Kempf, B. Andree, and R. Zweigerdt, "Large-scale production of human pluripotent stem cell derived cardiomyocytes," Adv. Drug Deliv. Rev. **96**, 18–30 (2016).
25. Z. Vukadinovic-Nikolic, B. Andrée, S. E. Dorfman, M. Pflaum, T. Horvath, M. Lux, L. Venturini, A. Bär, G. Kensah, A. R. Lara, I. Tudorache, S. Cebotari, D. Hilfiker-Kleiner, A. Haverich, and A. Hilfiker, "Generation of Bioartificial Heart Tissue by Combining a Three-Dimensional Gel-Based Cardiac Construct with Decellularized Small Intestinal Submucosa," Tissue Eng. Part A **20**(3-4), 799–809 (2013).
26. H. Kempf, R. Olmer, C. Kropp, M. Rückert, M. Jara-Avaca, D. Robles-Diaz, A. Franke, D. A. Elliott, D. Wojciechowski, M. Fischer, A. Roa Lara, G. Kensah, I. Gruh, A. Haverich, U. Martin, and R. Zweigerdt, "Controlling expansion and cardiomyogenic differentiation of human pluripotent stem cells in scalable suspension culture," Stem Cell Rep. **3**(6), 1132–1146 (2014).
27. K. Schwanke, S. Merkert, H. Kempf, S. Hartung, M. Jara-Avaca, C. Templin, G. Göhring, A. Haverich, U. Martin, and R. Zweigerdt, "Fast and efficient multitransgenic modification of human pluripotent stem cells," Hum. Gene Ther. Methods **25**(2), 136–153 (2014).
28. C. A. Schneider, W. S. Rasband, and K. W. Eliceiri, "NIH Image to ImageJ: 25 years of image analysis," Nat. Methods **9**(7), 671–675 (2012).
29. K. R. Gee, K. A. Brown, W. N. Chen, J. Bishop-Stewart, D. Gray, and I. Johnson, "Chemical and physiological characterization of fluo-4 Ca(2+)-indicator dyes," Cell Calcium **27**(2), 97–106 (2000).
30. D. M. Bers, "Calcium Fluxes Involved in Control of Cardiac Myocyte Contraction," Circ. Res. **87**(4), 275–281 (2000).
31. G. Bisker and D. Yelin, "Noble-metal nanoparticles and short pulses for nanomanipulations: theoretical analysis," J. Opt. Soc. Am. B **29**(6), 1383 (2012).
32. E. Lukianova-Hleb, Y. Hu, L. Latterini, L. Tarpani, S. Lee, R. A. Drezek, J. H. Hafner, and D. O. Lapotko, "Plasmonic nanobubbles as transient vapor nanobubbles generated around plasmonic nanoparticles," ACS Nano **4**(4), 2109–2123 (2010).
33. J.-C. Kim, M.-J. Son, K. P. Subedi, D. H. Kim, and S.-H. Woo, "IP3-induced cytosolic and nuclear Ca2+ signals in HL-1 atrial myocytes: possible role of IP3 receptor subtypes," Mol. Cells **29**(4), 387–395 (2010).
34. J.-C. Kim, M.-J. Son, K. P. Subedi, Y. Li, J. R. Ahn, and S.-H. Woo, "Atrial local Ca2+ signaling and inositol 1,4,5-trisphosphate receptors," Prog. Biophys. Mol. Biol. **103**(1), 59–70 (2010).
35. V. Tseeb, M. Suzuki, K. Oyama, K. Iwai, and S. Ishiwata, "Highly thermosensitive Ca dynamics in a HeLa cell through IP(3) receptors," HFSP J. **3**(2), 117–123 (2009).
36. L. Leybaert and M. J. Sanderson, "Intercellular Ca(2+) waves: mechanisms and function," Physiol. Rev. **92**(3), 1359–1392 (2012).
37. W. C. Claycomb, N. A. Lanson, Jr., B. S. Stallworth, D. B. Egeland, J. B. Delcarpio, A. Bahinski, and N. J. Izzo, Jr., "HL-1 cells: a cardiac muscle cell line that contracts and retains phenotypic characteristics of the adult cardiomyocyte," Proc. Natl. Acad. Sci. U.S.A. **95**(6), 2979–2984 (1998).

Biomedical Optics EXPRESS

38. J. C. Sáez, J. A. Connor, D. C. Spray, and M. V. Bennett, "Hepatocyte gap junctions are permeable to the second messenger, inositol 1,4,5-trisphosphate, and to calcium ions," Proc. Natl. Acad. Sci. U.S.A. **86**(8), 2708–2712 (1989).
39. J. P. Leonard and M. M. Salpeter, "Agonist-induced myopathy at the neuromuscular junction is mediated by calcium," J. Cell Biol. **82**(3), 811–819 (1979).
40. S. Orrenius, B. Zhivotovsky, and P. Nicotera, "Regulation of cell death: the calcium-apoptosis link," Nat. Rev. Mol. Cell Biol. **4**(7), 552–565 (2003).
41. P. Lipp, M. Laine, S. C. Tovey, K. M. Burrell, M. J. Berridge, W. Li, and M. D. Bootman, "Functional InsP3 receptors that may modulate excitation-contraction coupling in the heart," Curr. Biol. **10**(15), 939–942 (2000).
42. D. Luo, D. Yang, X. Lan, K. Li, X. Li, J. Chen, Y. Zhang, R.-P. Xiao, Q. Han, and H. Cheng, "Nuclear Ca2+ sparks and waves mediated by inositol 1,4,5-trisphosphate receptors in neonatal rat cardiomyocytes," Cell Calcium **43**(2), 165–174 (2008).
43. M. Schomaker, D. Killian, S. Willenbrock, D. Heinemann, S. Kalies, A. Ngezahayo, I. Nolte, T. Ripken, C. Junghanß, H. Meyer, H. Murua Escobar, and A. Heisterkamp, "Biophysical effects in off-resonant gold nanoparticle mediated (GNOME) laser transfection of cell lines, primary- and stem cells using fs laser pulses," J. Biophotonics **8**(8), 646–658 (2015).
44. J. L. Carvalho-de-Souza, J. S. Treger, B. Dang, S. B. H. Kent, D. R. Pepperberg, and F. Bezanilla, "Photosensitivity of neurons enabled by cell-targeted gold nanoparticles," Neuron **86**(1), 207–217 (2015).
45. N. I. Smith, S. Iwanaga, T. Beppu, K. Fujita, O. Nakamura, and S. Kawata, "Photostimulation of two types of Ca 2+ waves in rat pheochromocytoma PC12 cells by ultrashort pulsed near-infrared laser irradiation," Laser Phys. Lett. **3**(3), 154–161 (2006).
46. G. M. Dittami, S. M. Rajguru, R. A. Lasher, R. W. Hitchcock, and R. D. Rabbitt, "Intracellular calcium transients evoked by pulsed infrared radiation in neonatal cardiomyocytes," J. Physiol. **589**(6), 1295–1306 (2011).
47. C. Robertson, D. D. Tran, and S. C. George, "Concise review: maturation phases of human pluripotent stem cell-derived cardiomyocytes," Stem Cells **31**(5), 829–837 (2013).

1. Introduction

Various applications in the biomedical research field have started to combine gold nanoparticles with laser irradiation. These include techniques for the sensitive detection of molecules [1,2] and methods for cell treatment or manipulation, such as photothermal therapy [1,3,4] or cell transfection [5–8]. Yet, it has to be determined if the same principle would be applicable to a direct modification of molecule or cell function. While it has already been shown that nanoparticles and light can be applied for direct modification of DNA or antibodies, only few studies addressed the feasibility of this combination for stimulation of native cell functions, for instance, neuronal excitation [4,9–11]. Our study presents pioneering work and principal results to use light and nanoparticles for modulation of cardiac activity.

The human heart and other muscles are heterologous cell populations, which consist of a variety of cell types [12]. Therefore, it is difficult to induce a given activation threshold in a single cell type, a limited number of cells, or a specific cell region [12,13]. Optical methods accomplish cell-specific selectivity by spatially selective illumination. Recently, four important concepts for induction of cardiac activity using optical methods were demonstrated [14–17].

Two of these concepts utilize the framework of optogenetics. This requires that irradiated cells express light sensitive ion channels, for example, channelrhodopsin-2 [18]. Upon irradiation with blue light, channelrhodopsin-2 undergoes a conformational change and cations can enter the cell through this channel. Bruegmann et al. demonstrated light-induced activation of cardiomyocytes using channelrhodopsin-2. The induced ion exchange and depolarization altered the calcium homeostasis and cardiomyocyte beating [14]. The approach was successfully used *in vitro* and *in vivo*. Jia et al. employed another strategy in which a non-excitable donor cell was genetically modified to express channelrhodopsin-2 [15]. This cell was attached to host cardiomyocytes, such that the cells were interconnected via gap junctions. Upon irradiation, cations entered the non-excitable cell and the interconnected cardiomyocyte was activated. This tandem cell unit approach was successfully tested *in vitro* [15].

The third and fourth approach do not require the use of optogenetics. Accordingly, transgenic expression of channelrhodopsin-2 or other light sensitive channels is avoided.

Biomedical Optics EXPRESS

Smith et al. employed a femtosecond laser for direct stimulation of cardiomyocytes, connected to changes in intracellular calcium [16]. A former study by the same group irradiated different parts of cells by focused femtosecond laser pulses, in which calcium release upon irradiation of cytoplasm, or calcium inflow and release by optoporation of the membrane was observed [19]. Consequently, intracellular and extracellular calcium sources would possibly contribute to cardiomyocyte activation. A major disadvantage of this approach is the required membrane-focusing of single cells, which is time consuming and does not allow targeting more than a single cell simultaneously. The fourth optical approach employed a pulsed infrared diode laser at 1875 nm to pace quail embryonic heart [17]. The triggering was probably caused by the induced temperature gradient.

In this study, we followed the principle idea of Smith et al. with the aim of simultaneously addressing many cells. Therefore, we used a combination of gold nanoparticles and pulsed laser irradiation. We applied 200 nm unmodified gold nanoparticles at concentrations of about ten to thirty particles per cell, which are considered as non-toxic [6,20]. The nanoparticles attach unspecifically to the membrane through sedimentation. Irradiation of the particles with a laser system operating at 532 nm and a pulse length of 850 ps led to heating of the particles of several hundred K [5]. Based on our previous work, which analyzed different cell parameters including calcium exchange during gold nanoparticle mediated laser manipulation, we aimed to achieve cardiac activity [21]. We tested the stimulation of a cardiac myocyte cell line (HL-1 cells) in calcium containing and calcium free Hanks' Balanced Salt Solution (HBSS) using gold nanoparticle mediated laser stimulation, since calcium has a central role in cardiomyocyte activity as described in the four studies from above. Additionally, in human embryonic stem cell (hESC-) derived cardiomyocytes the calcium concentration has influence during electrical pacing [22]. Consequently, we extended our results to native rat cardiomyocytes and to cardiomyocytes derived from hESCs, which represent a valuable model of human heart muscle cells in a dish [23,24], to test our novel idea of myocyte stimulation.

2. Methods

2.1 Cell culture

HL-1 cells were cultured in Claycomb medium (Sigma-Aldrich) supplemented with 10% fetal bovine serum (Merck, Germany), 100 µg/ml penicillin and streptomycin (Merck, Germany), 0.1 mM norepinephrine (Sigma-Aldrich) and 2 mM L-glutamine (Sigma-Aldrich) at 37°C in a humidified 5% CO_2 atmosphere. Before plating cells, culture dishes were coated with a solution of 5 µg/ml fibronectin (Sigma-Aldrich) in 0.02% gelatin in water for one hour at 37°C.

Neonatal rat cardiomyocytes were isolated as previously described [25] and cultured in DMEM/M199 medium supplemented with 10% fetal bovine serum, 5% horse serum, 1% penicillin and streptomycin and 1% L-glutamine at 37°C in a humidified 5% CO_2 atmosphere.

hESC-derived cardiomyocytes were generated as described [23,26]. Briefly, hES3-aMHCneoPGKhygro transgenic cells [27] were seeded in mTeSR1 medium (Stemcell Technologies) into Erlenmeyer flasks (BD Falcon) rotated at 60 revolutions/min to form aggregates. Differentiation was induced in RB- medium (RPMI 1640 with B27 supplement without insulin; Life Technologies, USA) supplemented with 7.5 µM CHIR99021 (synthesized by the Institute of Organic Chemistry, Leibniz University Hannover or purchased from Millipore) for 24 hours before being replaced by RB- medium supplemented with 5 µM IWP2 (Tocris) for 48 hours. On day 3 and 5 the medium was changed to RB- only and from day 7 onwards cells were maintained in RB + (RPMI 1640 with B27 supplement including insulin; Life Technologies). The resulting cardiomyocyte aggregates were dissociated using the Miltenyi gentleMACS Dissociator and Kit (Miltenyi Biotec) and seeded onto fibronectin-coated 35 mm glass bottom microdishes (Ibidi) and cultured in RB +

Biomedical Optics EXPRESS

medium supplemented with 1% penicillin and streptomycin at 37°C in a humidified 5% CO_2 atmosphere.

Spherical gold nanoparticles with a diameter of 200 nm (PGO200, Kisker, Germany) were added to cells for three hours. Sedimentation leads to unspecific attachment of the particles to the cell membrane. As validated in former studies, a concentration of 0.5 µg/cm^2 corresponds to about ten to thirty particles per cell [5,6,21]. A laser beam with a previously determined spot diameter of 80 µm irradiated the cells, which were placed on an epifluorescence microscope, from the top. A more detailed description of the setup is given in [21]. All applied laser parameters are stated in the text. The repetition rate of the laser system was 20.25 kHz at a wavelength of 532 nm.

2.2 Labeling of cells with the calcium indicator Fluo-4

After sedimentation of the gold nanoparticles, cardiomyocytes were washed with OptiMEM medium (Life Technologies) three times and subsequently incubated for 20 minutes at 37°C and 5% CO_2 with 1.8 µM Fluo-4, AM (Life Technologies) diluted in OptiMEM medium. Cardiomyocytes were incubated in OptiMEM medium without dye for another 20 minutes before the medium was replaced with either calcium free or calcium containing buffer. In detail, three different calcium buffers were used and are designated in the text as follows: HBSS-Ca^{2+} (138 mM NaCl, 5.4 mM KCl, 441 µM KH_2PO_4, 337 µM Na_2HPO_4, 4.17 mM $NaHCO_3$, 5.55 mM $C_6H_{12}O_6$, 0 mM Ca^{2+}), HBSS + Ca^{2+} (with additional 406 µM $MgSO_4$–$7H_2O$, 492 µM $MgCl_2$–$6H_2O$ and 1.26 mM $CaCl_2$), HBSS + hCa^{2+} (with 10 mM $CaCl_2$ instead of 1.26 mM). Laser treatment was applied immediately after addition of the respective calcium buffer.

2.3 Laser stimulation and imaging

To stimulate calcium signaling in HL-1 cells, radiant exposures of 8 mJ/cm^2, 15 mJ/cm^2, 21 mJ/cm^2, and 27 mJ/cm^2 and irradiation times of 10 ms or 20 ms were applied. With an exposure time of 200 ms and a frame rate of 5 fps, Fluo-4 fluorescence intensities were detected 2 s pre and over a time span of 38 s post laser stimulation using a 63x objective (Plan-Apochromat, Zeiss). At least n = 10 directly irradiated HL-1 cells in HBSS + Ca^{2+} and HBSS-Ca^{2+} were investigated for each radiant exposure and irradiation time.

Calcium signaling in hESC-derived cardiomyocytes was stimulated with a radiant exposure of 15 mJ/cm^2 and an irradiation time of 10 ms on day two in culture. With an exposure time of 200 ms and a frame rate of 5 fps, Fluo-4 fluorescence intensities of at least n = 15 cardiomyocytes in HBSS + Ca^{2+} and HBSS-Ca^{2+} were detected over a time span of 80 s (30 s pre and 50 s post laser stimulation) using a 63x objective. Another n = 10 cardiomyocytes in HBSS + Ca^{2+} were investigated using a 10x objective (Fluar, Zeiss). Fluo-4 fluorescence intensities were detected over a time span of 40 s (15 s pre and 25 s post laser irradiation) with an exposure time of 200 ms and a frame rate of 5 fps.

Cell contractions of at least n = 7 rat neonatal cardiomyocytes in HBSS-Ca^{2+}, HBSS + Ca^{2+}, and HBSS + hCa^{2+} were investigated on day seven in culture. With an exposure time of 50 ms and a frame rate of 12.8 fps using a 63x objective, bright field microscopy images were captured over a time span of 80 s with laser irradiation (radiant exposure 8 mJ/cm^2 and 10 ms irradiation time) at every 15.6 s.

Cell contractions of at least n = 25 hESC-derived cardiomyocytes in HBSS-Ca^{2+}, HBSS + Ca^{2+}, and HBSS + hCa^{2+} were investigated on day eight to ten in culture after dissociation. With an exposure time of 50 ms and a frame rate of 12.8 fps using a 63x objective, bright field microscopy images were captured over a time span of 80 s with laser irradiation (radiant exposure of 15 mJ/cm^2 and 10 ms irradiation time) at every 7.8 s.

Calcein AM (1 µM, Life Technologies) and Propidium Iodide (1 µM, Life Technologies) double staining was used to determine cell viability of hESC-derived cardiomyocytes one

Biomedical Optics EXPRESS

hour after laser treatment. Calcein and Propidium Iodide stained cells within the irradiated area were counted.

2.4 Image analysis

To analyze the cardiomyocytes' fluorescence signals, every cell in the field of view of each stack of images was selected manually using the selection tool of ImageJ [28]. Additionally, a background value without cells was determined for each field of view. The mean gray value within each selection corrected for background corresponds to the mean Fluo-4 fluorescence intensity of this cell and was obtained for each image of the stack using ImageJ. The normalized Fluo-4 intensity ($\Delta F/F_0$) was graphically represented using the software OriginLab, with F_0 being the initial fluorescence. Oscillation frequencies were determined using OriginLab's peak analysis tool.

Bright field images were analyzed using ImageJ. The first image of a stack was subtracted from the entire stack, so that cell contractions were visible by high black/white-contrasts. A significant region of interest was selected manually and mean gray values of the selection were obtained by ImageJ for every image of the stack. A graphic representation of the mean gray values in dependence of time was obtained using OriginLab with every peak corresponding to one contraction. Contraction frequencies were determined using OriginLab's peak analysis tool. Every graphic plot was compared with the original stack of captured images to identify possible artifacts that might affect the mean gray values. Visualizations are uploaded as separate files.

3. Results

3.1 Gold nanoparticle mediated laser stimulation induces laser parameter dependent calcium oscillations in HL-1 cells

To study the general applicability of gold nanoparticle mediated laser manipulation for cell excitation in heart muscle cells, we examined the calcium response in HL-1 cells using the fluorescent calcium indicator Fluo-4. Fluo-4 binds to free calcium ions, which leads to an increase of its fluorescence signal [29]. Thus, the detected fluorescence level correlates with the concentration of intracellular calcium ions. We applied different radiant exposures and irradiation times to determine the best suited laser parameters for stimulation.

The laser stimulation induced three different events in HL-1 cells. These could be distinguished in: 1) a significant increase of Fluo-4 intensity immediately after irradiation, followed by a constant high intensity over the entire measurement (*calcium shock*), 2) no change of fluorescence (*no response*), and 3) alternating in- and decrease of Fluo-4 intensity (*calcium oscillation*). Directly irradiated cells showed a different calcium response compared to those localized in the surrounding area of the laser spot. Thus, we also divided the images in three regions for the analysis: 1) within the laser spot, 2) at the periphery of the laser spot, and 3) outside of the spot. A cell's localization was categorized as at the periphery of the laser spot, if it was localized partly within and partly outside of the laser spot (see Fig. 1(a)).

Due to their signaling characteristics, intracellular calcium oscillations can serve as indicator of cell contractions. Thus, intercellular calcium waves/oscillations indicated the propagation of a signal, which would possibly induce contraction of neighboring cells. Therefore, different laser parameters were tested to determine, which parameters induced the highest number of HL-1 cells responding with intercellular calcium oscillations throughout all regions (see Fig. 1(b)).

In HBSS + Ca^{2+}, intracellular calcium oscillations were observed in 39 +/– 8% to 65 +/– 6% of HL-1 cells in the area outside of the laser spot for all radiant exposures and irradiation times. Within the laser spot, calcium levels increased rapidly and remained at an elevated level (calcium shock) in more than 80% of the HL-1 cells for radiant exposures of 21 mJ/cm^2 and 27 mJ/cm^2 (see Fig. 2(a), 2(b) and Visualization 1). The highest percentage of calcium

Biomedical Optics EXPRESS

oscillations cumulated in all regions was achieved for a radiant exposure of 15 mJ/cm^2 and 20 ms irradiation time. In this case, calcium oscillations were present in 34 +/– 8% of cells within the laser spot, 62 +/– 9% at the periphery of the laser spot and 60 +/– 6% of the cells outside of the laser spot. 30 +/– 7% of the directly irradiated HL-1 cells responded with calcium shock. The frequency of the calcium oscillations varied from 0.25 Hz to 0.5 Hz for low radiant exposures (8 mJ/cm^2 and 15 mJ/cm^2), and 0.5 Hz to 1 Hz for higher radiant exposures (21 mJ/cm^2 and 27 mJ/cm^2; see Fig. 2(c)). All laser induced calcium responses in HL-1 cells were predominantly determined by the radiant exposure rather than the irradiation times applied, which did not show any significant effects. No change in the Fluo-4 intensity was observed in HL-1 cells, which were not treated with gold nanoparticles for any applied radiant exposure and irradiation time (see Fig. 8).

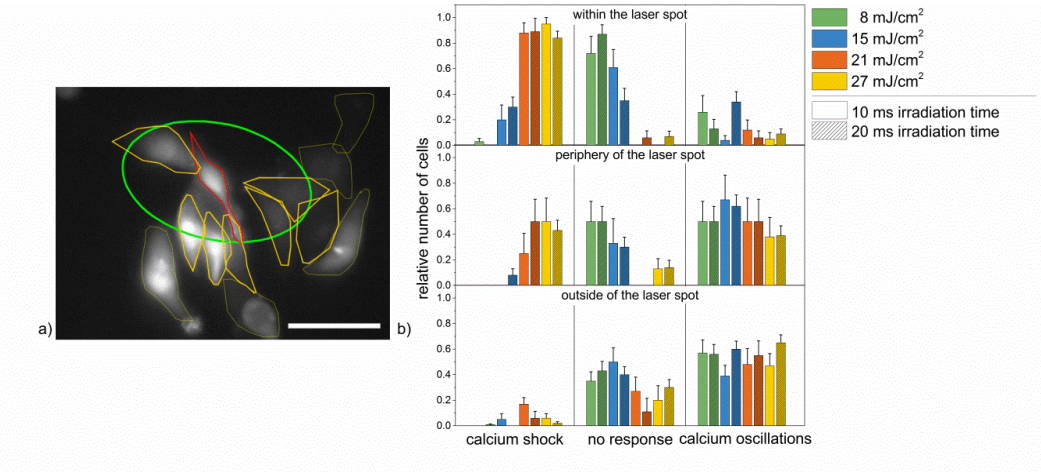

Fig. 1. Calcium responses of HL-1 cells in HBSS + Ca^{2+} after laser stimulation with different radiant exposures and irradiation times for the three considered regions. (a): Distribution of cells within the laser spot (*red selection*), at the periphery of the laser spot (*orange selection*) and outside of the laser spot (*yellow selection*) with the laser spot being marked green. Scale bar: 40 µm. (b): Relative frequency of occurrence of the three different calcium responses shown in HL-1 cells in HBSS + Ca^{2+} buffer after laser stimulation of cells within the laser spot (*top*), at the periphery of the laser spot (*middle*) and outside of the laser spot (*bottom*). Accumulated over all three areas, calcium oscillations occurred most frequently with a radiant exposure of 15 mJ/cm^2 and 20 ms irradiation time. Data represents the mean + SEM of at least n = 10 irradiated cells.

Biomedical Optics EXPRESS

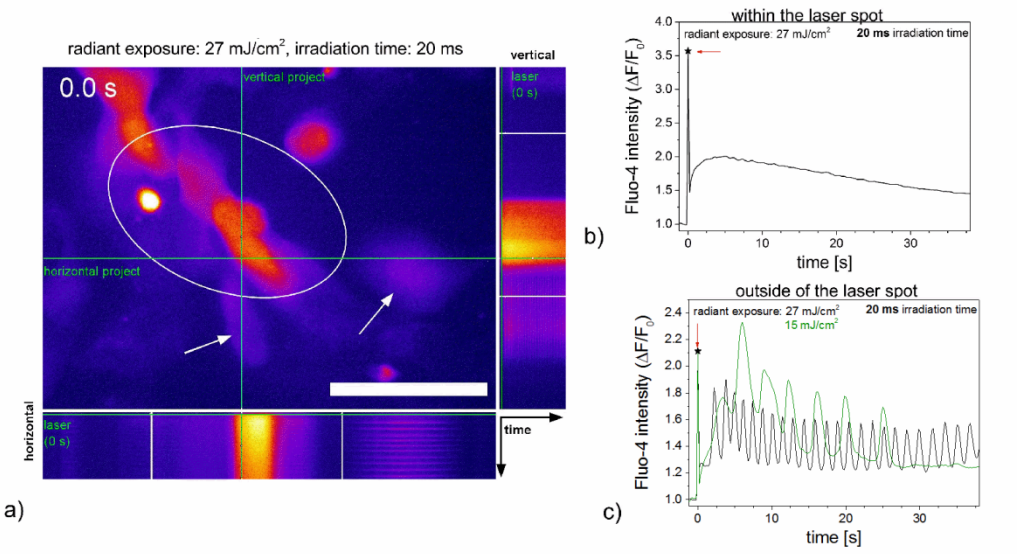

Fig. 2. Laser induced calcium responses of HL-1 cells in HBSS + Ca^{2+} after laser stimulation. An orthogonal projection (time plotted along the green lines) of Visualization 1 shows different effects of the laser stimulation on calcium signaling with a radiant exposure of 27 mJ/cm^2 in HL-1 cells (a). In both projections, a calcium shock can be observed over time for the cell, which is in the laser treated area after laser application. Calcium oscillations are visible at the periphery or outside of the laser spot. Scale bar 50 µm. Panels b) and c) show the quantified response of a single representative cell. Laser irradiation occurred at 0 s (arrow pointing to asterisk) with the laser spot being located within the marked area. Cells within the laser spot mostly responded with a calcium shock, while cells not directly irradiated often exhibited calcium oscillations after laser treatment. Please refer to Visualization 1 for a time series of subfigures a) to c).

3.2 Dependence of gold nanoparticle mediated laser stimulation induced calcium oscillations in HL-1 cells on the extracellular calcium level

To investigate the influence of extracellular calcium that might enter the cell during perforation, calcium free HBSS buffer was applied in another experimental series. For an irradiation time of 20 ms, two different radiant exposures, which yielded a high amount of calcium shock and calcium oscillations in cells after laser irradiation (15 mJ/cm^2 and 27 mJ/cm^2), were employed (see Fig. 3). The location of the cells during irradiation and the radiant exposure resulted in the main influence on the calcium response of the cells. The occurrence of induced calcium oscillations in calcium free buffer was up to 18% lower than in calcium containing buffer. However, this was not statistically significant for any pair of radiant exposures in a single location ($p>0.23$, t-test).

Biomedical Optics EXPRESS

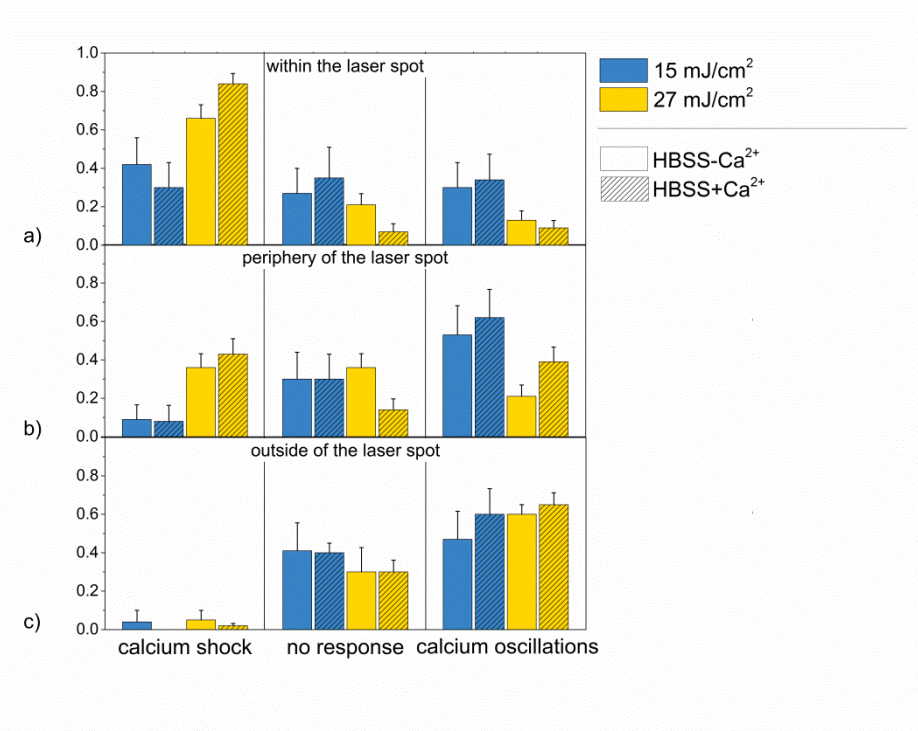

Fig. 3. Calcium responses of HL-1 cells in Ca^{2+} containing and Ca^{2+} free buffer after laser stimulation. Relative frequency of occurrence of the three different calcium responses in HL-1 cells in HBSS + Ca^{2+} and HBSS-Ca^{2} after laser stimulation of cells within the laser spot (a), at the periphery of the laser spot (b) and outside of the laser spot (c) for an irradiation time of 20 ms and radiant exposures of 15 mJ/cm^2 and 27 mJ/cm^2. Data represents the mean + SEM of at least n = 10 irradiated cells.

3.3 Gold nanoparticle mediated laser stimulation affects contractile behavior of neonatal rat cardiomyocytes

Based on the observed calcium oscillations in HL-1 cells, we aimed to test gold nanoparticle mediated laser stimulation for primary cardiomyocytes. In particular, we were interested in cell contractions, as calcium signaling contributes significantly to the contraction of cardiomyocytes. To determine if gold nanoparticle mediated laser manipulation can induce contractions in cardiomyocytes, we investigated its effects on neonatal rat cardiomyocytes *in vitro*. A radiant exposure of 8 mJ/cm^2 and an irradiation time of 10 ms were used in the three buffers (HBSS-Ca^{2+}, HBSS + Ca^{2+}, and HBSS + hCa^{2+}). Cells were treated on the seventh day in culture and analyzed using bright field microscopy.

Before laser irradiation, cardiomyocytes in all media showed a contractile behavior with frequencies between 0.1 Hz and 3 Hz. Cardiomyocytes in HBSS-Ca^{2+} exhibited contractions with steady frequencies, independent of laser treatment (see Fig. 4(a)). Laser stimulation affected especially cardiomyocytes in HBSS + Ca^{2+} by increasing their frequencies of contraction by an average of 50%. An individual cell in HBSS + Ca^{2+}, whose contractility is exemplarily represented in Fig. 4(b) (see also Visualization 2), showed a steady contractile rhythm before laser stimulation.

Biomedical Optics EXPRESS

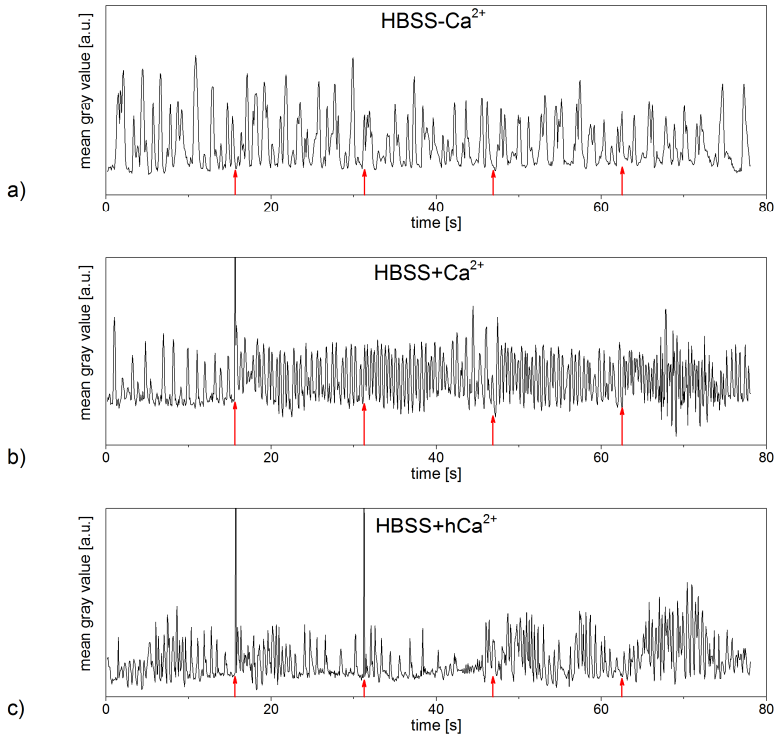

Fig. 4. Contractions of neonatal rat cardiomyocytes pre and post laser stimulation with a radiant exposure of 8 mJ/cm^2 and an irradiation time of 10 ms. While the laser stimulation did not affect the contractile behavior of the examined cardiomyocyte in HBSS-Ca^{2+} (a), it induced significant increases of the contraction frequency in cardiomyocytes in HBSS + Ca^{2+} (b) (referring to Visualization 2). Cardiomyocytes in HBSS + hCa^{2+} exhibited higher contraction frequencies after laser treatment as well (c) (referring to Visualization 3). Laser irradiation occurred every 15.6 s (red arrows), every peak represents one contraction of the examined cardiomyocyte. Data shown represents the exemplary contractile behavior of one single out of at least n = 7 examined cells or set of cells in HBSS-Ca^{2+}, HBSS + Ca^{2+} and HBSS + hCa^{2+}, respectively. Narrow peaks are laser light detected by the camera if it was coincident with the frame acquisition.

Immediately after irradiation, the number of contractions increased significantly before slowly decreasing again within a time span of 15 s. On average, laser stimulation induced an increase in frequency of 0.83 +/– 0.25 Hz, which is equivalent to 57 +/– 16% (averaged over a time span of 3.9 s).

Gold nanoparticle mediated laser manipulation mostly showed no effects on cardiomyocytes in HBSS + hCa^{2+}, but rarely induced a significant increase in the cells' frequency of contraction. Figure 4(c) represents the contractile behavior of an exemplary cell in HBSS + hCa^{2+} (see also Visualization 3). Before laser irradiation, the cardiomyocyte's rhythm of contraction alternated strongly, exhibiting frequencies from 0.5 Hz to 1.8 Hz (averaged over a time span of 3.9 s). Immediately after laser stimulation, the frequency of contraction increased by a minimum of 80% and a maximum of 150% in respect to the recorded frequency averaged over the last 3.9 s before laser irradiation. As the examined cardiomyocytes' rhythms of contraction were unsteady even before laser treatment, its effects on the cells' contractile behavior cannot be stated conclusively at this point.

No laser induced effects on cardiomyocytes' contractility were observed in cells not treated with gold nanoparticles (see Fig. 8).

Biomedical Optics EXPRESS

3.4 Effects of gold nanoparticle mediated laser stimulation on human embryonic stem cell derived cardiomyocytes

The effects of gold nanoparticle mediated laser stimulation on hESC-derived cardiomyocytes', which represent a valuable model for regenerative therapies, calcium signaling as well as on their contractile behavior were investigated using fluorescence and bright field imaging. For all experiments, a radiant exposure of 15 mJ/cm^2 and an irradiation time of 10 ms were applied.

We first confirmed that this radiant exposure and irradiation time did not have any significant impact on cell viability (see Fig. 5). We obtained viabilities of >80% in all three different buffers using a live-dead staining with Calcein and Propidium Iodide. This is in good agreement with our previous studies [21].

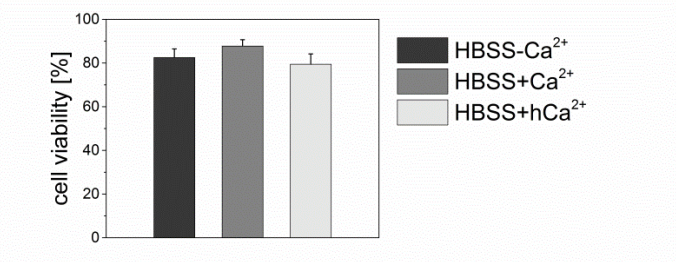

Fig. 5. Cell viability of hESC-derived cardiomyocytes in HBSS-Ca^{2+}, HBSS + Ca^{2+} and HBSS + hCa^{2+}, respectively, one hour after multiple laser irradiations with a radiant exposure of 15 mJ/cm^2 and an irradiation time of 10 ms. In all three buffers, cell viability is >80%. Data presents the mean + SEM of at least n = 20 irradiated cells.

Calcium signals in hESC-derived cardiomyocytes were detected with the fluorescent calcium indicator Fluo-4 (as for HL-1 cells) and recorded on day two in culture. All investigated cardiomyocytes in HBSS + Ca^{2+} exhibited calcium oscillations before laser treatment. Within 10 s post laser treatment, spatially simultaneous intercellular calcium oscillations were observed in 50% of the cardiomyocytes in HBSS-Ca^{2+}. The other half of the examined cardiomyocytes in HBSS-Ca^{2+} did neither show spontaneous nor laser induced calcium oscillations. Directly irradiated cells responded to laser stimulation with a calcium shock, while in adherent cardiomyocytes not located within the laser spot, a calcium spike occurring immediately after laser irradiation was recorded in some cases (see Fig. 6(a), 6(b) and Visualization 4). hESC-derived cardiomyocytes not treated with gold nanoparticles did not show a laser induced calcium response (see Fig. 8).

Biomedical Optics EXPRESS

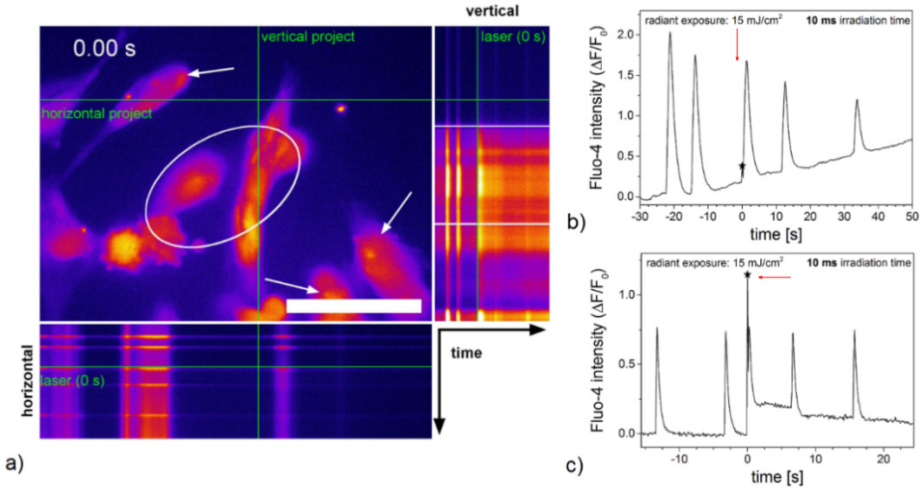

Fig. 6. Calcium signaling in hESC-derived cardiomyocytes in HBSS + Ca^{2+} pre and post laser stimulation with a radiant exposure of 15 mJ/cm^2 and an irradiation time of 10 ms. An orthogonal projection of Visualization 4 indicates the effects of laser stimulation on calcium signaling in hESC-derived cardiomyocytes (a). Scale bar 50 µm. Laser irradiation occurred at 0 s with the laser spot being located within the marked area. The relative fluorescence intensity of cardiomyocytes located outside of the laser spot (marked by arrows) shows the occurrence of a calcium oscillation immediately after laser treatment (arrow and asterisk) (b). Considering a larger field of view using the 10x objective, all hESC-derived cardiomyocytes outside of the laser spot exhibited an additional, simultaneously occurring calcium oscillation immediately after laser treatment (c). Graph (c) refers to Visualization 5. Data shown refers to a single irradiated hESC-derived cardiomyocyte for all graphs out of n = 15 (63x objective) and n = 10 (10x objective) irradiated cells.

We further investigated the calcium oscillations over a long spatial distance using a 10x objective. hESC-derived cardiomyocytes in HBSS + Ca^{2+} exhibited simultaneous calcium oscillations in all cells within the field of view with a steady frequency. No effects of gold nanoparticle mediated laser stimulation on calcium signaling in cardiomyocytes were detected in most the recordings. In >30%, hESC-derived cardiomyocytes in the entire field of view outside of the laser spot showed an additional, simultaneously occurring calcium spike immediately after laser irradiation (see Fig. 6(c) and Visualization 5), while in directly irradiated cells, a calcium shock was observable.

On day eight to ten in culture, we investigated effects of laser stimulation on hESC-derived cardiomyocytes' contractile behavior. For cardiomyocytes in HBSS-Ca^{2+}, either no contractions (neither spontaneous nor post laser stimulation) were observed or the laser irradiation led to inhibition of contractions (see Fig. 7(a)). hESC-derived cardiomyocytes in HBSS + Ca^{2+} showed a steady contracting rhythm not affected by the laser treatment (see Fig. 7(b)). Out of 30 treated cells, few cells (< 30%) showed an alteration of the contraction frequency in HBSS + hCa^{2+}. Figure 7(c) represents the contractile behavior of one exemplary cell affected by laser treatment, referring to supplementary Visualization 6. Immediately after contraction and before full relaxation occurred, the irradiation of the cardiomyocyte induced another contraction of the cell. This was not observed in any investigated cardiomyocyte as spontaneous behavior. The second as well as third laser irradiation also caused the cell to contract. For repeated laser irradiations, this correlation between stimulation and cell contraction vanished.

No effects of laser stimulation were observed in hESC-derived cardiomyocytes not treated with gold nanoparticles (see Fig. 8).

Biomedical Optics EXPRESS

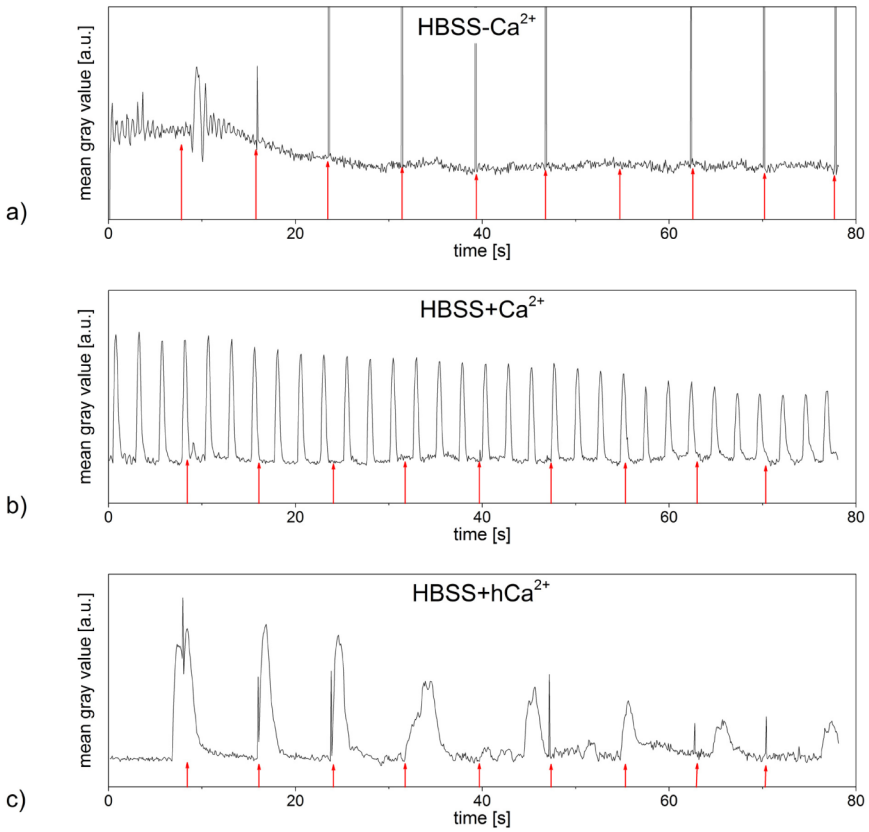

Fig. 7. Contractions of hESC-derived cardiomyocytes pre and post laser stimulation with a radiant exposure of 15 mJ/cm^2 and an irradiation time of 10 ms. The laser treatment stopped contractions of the examined cardiomyocyte in HBSS-Ca^{2+} (a) and did not affect the contractile behavior of hESC-derived cardiomyocytes in HBSS + Ca^{2+} (b). In hESC-derived cardiomyocytes in HBSS + hCa^{2+}, some contractions occurred immediately after laser stimulation (c) (referring to Visualization 6). Laser irradiation occurred every 7.8 s (red arrows), every peak represents one contraction of the examined cardiomyocyte. Data shown represents the exemplary contractile behavior of one examined cell in HBSS-Ca^{2+}, HBSS + Ca^{2+} and HBSS + hCa^{2+}, respectively. Narrow peaks are laser light detected by the camera if it was coincident with the frame acquisition.

4. Discussion

In this study, we investigated the feasibility of gold nanoparticle mediated laser stimulation in the cardiac myocyte cell line HL-1, rat neonatal cardiomyocytes, and hESC-derived cardiomyocytes. As calcium ions contribute to the contractility of cardiomyocytes by binding to Troponin C, which leads to the activation of the myofilaments, we investigated calcium signaling in cardiomyocytes and contractions [30]. In all tested cells, reactions were only observed in the presence of gold nanoparticles (see Fig. 8)

Biomedical Optics EXPRESS

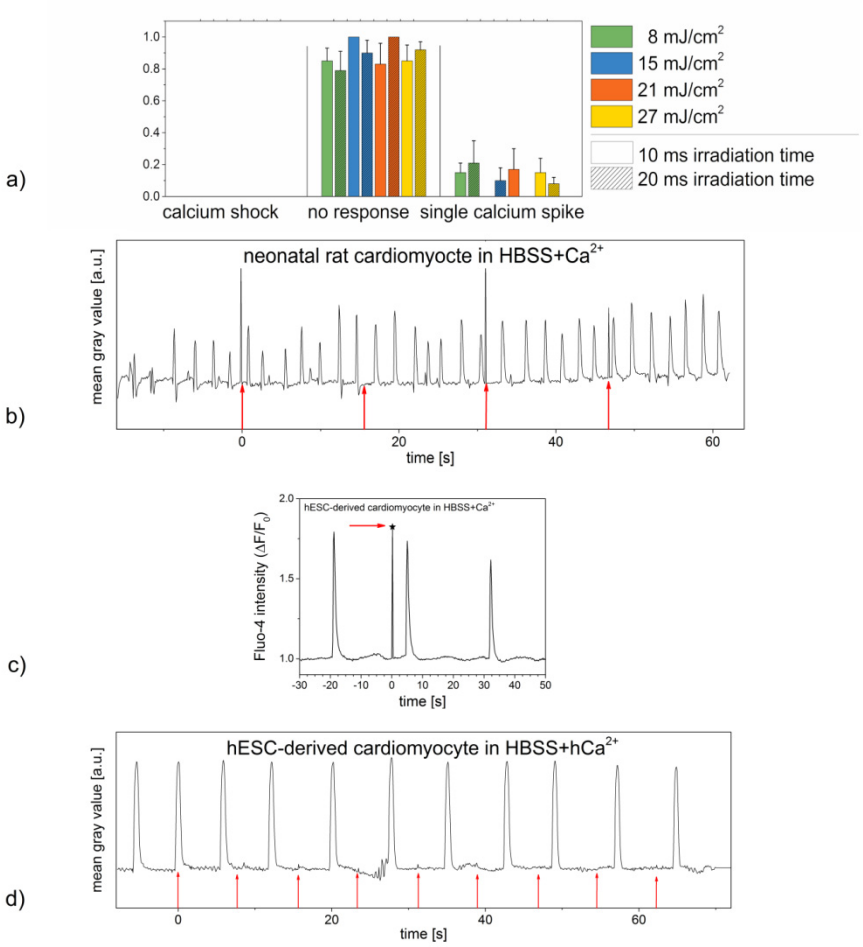

Fig. 8. Effects of laser irradiation on HL-1 cells, neonatal rat cardiomyocytes and hESC-derived cardiomyocytes not treated with gold nanoparticles. (a): Relative frequency of occurrence of the three different calcium responses shown in nanoparticle free HL-1 cells in HBSS + Ca^{2+} after laser stimulation with different radiant exposures and irradiation times. While the calcium level of most cells did not change after irradiation, single calcium spikes, which can occur spontaneously in HL-1 cells, were observed in a small number of cells. No steady intercellular calcium oscillations were observed. Data represents the mean + SEM of at least n = 8 irradiated cells. (b): Contractions of a nanoparticle free neonatal rat cardiomyocyte in HBSS + Ca^{2+} pre and post laser treatment with a radiant exposure of 8 mJ/cm^2 and an irradiation time of 10 ms. Laser irradiation occurred every 15.6 s (red arrows), every peak represents one contraction of the examined cardiomyocyte. No effects of laser irradiation on the cells' contractile behavior were observed. Data shown represents the exemplary contractile behavior of one single out of n = 10 examined cells or set of cells. (c): Calcium signaling in nanoparticle free hESC-derived cardiomyocytes in HBSS + Ca^{2+} pre and post laser stimulation with a radiant exposure of 15 mJ/cm^2 and an irradiation time of 10 ms. The laser irradiation (arrow and asterisk) did not affect the frequency of calcium oscillations or the overall calcium level represented by the relative fluorescence intensity. Data shown represents the calcium signaling of one single out of n = 8 irradiated cells. (d): Contractions of a nanoparticle free hESC-derived cardiomyocyte in HBSS + hCa^{2+} pre and post laser treatment with a radiant exposure of 15 mJ/cm^2 and an irradiation time of 10 ms. Laser irradiation occurred every 7.8 s (red arrows), every peak represents one contraction of the examined cardiomyocyte. No effects of laser irradiation on the cells' contractile behavior were observed. Data shown represents the exemplary contractile behavior of one single out of n = 10 examined cells or set of cells. Narrow peaks in (b), (c) and (d) are laser light detected by the camera if it was coincident with the frame acquisition.

Biomedical Optics EXPRESS

According to former studies, laser manipulation with the applied radiant exposures and irradiation times leads to heating of the gold nanoparticles by several hundred K [5,21,31]. The thermal process evokes a transient cell membrane permeabilization, probably through the photothermal formation of plasmonic nanobubbles [7,32]. This is different from multiphoton ionization during femtosecond cell stimulation as in the work of Smith et al. [16] and from spatio-temporal temperature gradients as in the study by Jenkins et al. [17].

The permeabilization enables influx of extracellular molecules and ions such as calcium, which possibly induces a rise of the intracellular calcium concentration ($[Ca^{2+}]_i$) in HL-1 cells. Calcium-induced calcium release might additionally yield a significant increase of the $[Ca^{2+}]_i$, explaining the high levels of calcium observed in HL-1 cells in HBSS + Ca^{2+} after laser irradiation. For HL-1 cells in HBSS-Ca^{2+}, no calcium influx could have occurred. It is therefor likely that the laser stimulation induced an intracellular signaling pathway that yields an increase in calcium. The IP_3 (inositol 4,5-triphosphate) pathway, which is present in HL-1 cells, can be initiated by membrane stress caused by heating or perforation [19,33–36]. By binding of IP_3 to IP_3 receptors, which are located in the membrane of the sarcoplasmic reticulum, calcium release to the cytoplasm can be induced. The intercellular propagation of calcium signals in HL-1 cells is likely based on signal transduction via gap junctions, which are expressed in HL-1 cells [37]. These are permeable for small molecules as calcium and IP_3 [38].

A prolonged, high intracellular calcium level, as observed in HL-1 cells showing a calcium shock, describes a perturbation of the calcium homeostasis. This often initiates cell death [39,40]. As shown recently, laser manipulation with high radiant exposures (comparable to 21 mJ/cm^2 and 27 mJ/cm^2) induces the formation of membrane blebs, a rearrangement of the f-actin cytoskeleton, and decreases viability in ZMTH3 cells [21]. Since the perforation event as localized membrane effect might be similar in HL-1 cells, the calcium shock in directly irradiated HL-1 cells could present a stress reaction and indicate emerging cell death. However, for the cell response, it is important to note that the cell type and calcium homeostasis of ZMTH3 and HL-1 cells are different. With the parameter set of 15 mJ/cm^2 and an irradiation time of 10 ms only a minor decrease in viability was observed in hESC-derived cardiomyocytes.

In neonatal rat cardiomyocytes, the intracellular IP_3 signaling pathway can trigger contractions by inducing a calcium release from the sarcoplasmic reticulum due to acute cell stress [41,42]. On this basis, we would expect but did not observe laser induced contractions in native rat cardiomyocytes in calcium free buffer. A possible stimulation of the production of IP_3 in the investigated cardiomyocytes might not have overcome the threshold for triggering a sufficient calcium release for additional contractions. Consequently, the effect of the laser treatment on the contraction frequency of cardiomyocytes in buffer with 1.26 mM and 10 mM calcium is probably owned to a transient cell membrane permeabilization as discussed for HL-1 cells. Moreover, a change in membrane potential caused by the permeabilization of the cell membrane could have induced the generation of action potentials [43]. The opening of voltage dependent ion channels upon stimulation would lead to a calcium influx into the cytoplasm, thereby increasing the $[Ca^{2+}]_i$. This effect occurs during gold nanoparticle mediated laser stimulation of neuronal activity [44]. Smith et al. stimulated neonatal rat cardiomyocytes by changing their membrane potential with direct irradiation of cells with a near infrared (780 nm) femtosecond laser [16,45]. Dittami et al. induced calcium oscillations as well as contractions in native cardiomyocytes with an infrared laser in their study and attributed this to heating effects [46]. The laser radiant exposure for neonatal rat cardiomyocytes was lower compared to HL-1 cells, because we aimed to apply the lowest radiant exposure possible. Next, to the different cell type this might also have caused a different reaction in the applied buffers, in particular in calcium free buffer.

As calcium serves as intracellular messenger contributing significantly to the contraction of cardiomyocytes, we expected to find a good correlation between the examined calcium

Biomedical Optics EXPRESS

signaling and contraction behavior of the hESC-derived cardiomyocytes. While gold nanoparticle mediated laser stimulation succeeded in inducing additional calcium spikes in cardiomyocytes in 1.26 mM calcium buffer, the cells' contractile behavior could not be affected. Possibly, the evoked calcium signals did not overcome a certain threshold to induce contractions in cardiomyocytes. An extracellular calcium concentration of 10 mM could evoke this effect. This is in agreement with studies by Dolnikov et al., who observed a significantly enhanced calcium response and contraction rate in embryoid bodies of hESC-derived cardiomyocytes in bath solutions of 4 mM and 6 mM but not 2 mM Ca^{2+} during electrical pacing [22]. Consequently, the main difference to neonatal rat cardiomyocytes can probably be attributed to the cells' maturation state, additional to the cell medium. In particular, calcium homeostasis and the influence/maturation of the sarcoplasmic reticulum are different in stem cell derived cardiomyocytes and also dependent on their age [22,47]. Also, the species of cell origin was different in the experiments.

5. Conclusion

In this study, we describe a novel approach to optically stimulate cardiomyocytes via pulsed laser irradiated gold nanoparticles. We found that intercellular calcium oscillations in HL-1 cells can be induced, in calcium containing and calcium free buffer. These are dependent on radiant exposure. Our investigations show, that the stimulation of rat neonatal cardiomyocytes as well as hESC-derived cardiomyocytes depends on the extracellular calcium concentration.

In contrast to optogenetic methods, which were used to stimulate myocardial activity in former studies, the method presented here does not necessitate any genetic modification, thereby sparing the use of transfection methods. Instead, gold nanoparticle mediated laser stimulation of cardiomyocytes uses the local heating effects due to laser-gold nanoparticle interactions thus providing a simpler cell stimulation approach.

Funding

This research was funded by the German Federal Ministry of Economics and Energy (BMWi) within the Promotion of Joint Industrial Research Programme (IGF) due to a decision of the German Bundestag. It was part of the research project 18129N by the Association for Research in Precision Mechanics, Optics and Medical Technology (F.O.M.) under the auspices of the German Federation of Industrial Research Associations (AiF). R. Zweigerdt, S. Kalies and A. Heisterkamp received funding from the German Research Foundation through the Cluster of Excellence REBIRTH (DFG EXC62/3); R. Zweigert received further funding from the DFG (ZW 64/4-1) and the German Ministry for Education and Science (BMBF; grant no. 13N12606). Parts of this work were carried out as an integral part of the BIOFABRICATION FOR NIFE Initiative, which is financially supported by the ministry of Lower Saxony and the Volkswagen Stiftung (BIOFABRICATION FOR NIFE: VWZN2860).